Physical Properties of Recombinant Apolipoprotein(a) and Its Association with LDL To Form an Lp(a)-like Complex†

Martin L. Phillips, Audra V. Lembertas, and Verne N. Schumaker*

Department of Chemistry and Biochemistry and the Molecular Biology Institute, University of California, Los Angeles, California 90024

Richard M. Lawn

Division of Cardiovascular Medicine, Falk Cardiovascular Research Center, Stanford University School of Medicine, Stanford, California 94305-5246

Steven J. Shire and Thomas F. Zioncheck

Department of Pharmaceutical Research and Development and the Metabolism Group, Genentech, Inc., South San Francisco, California 94080

Received September 14, 1992; Revised Manuscript Received January 22, 1993

ABSTRACT: Recombinant apolipoprotein(a) has been studied by hydrodynamic techniques and electron microscopy. Recombinant apo(a) was primarily a monomer in solution with an $s^0_{20,w}$ of 9.3 S, a $D_{20,w}$ of 2.29 ficks, and a molecular weight of 325 000 from sedimentation equilibrium and 318 000 from combining the sedimentation and diffusion coefficients. A small amount, approximately 10%, of the recombinant apo(a) was present as a high molecular weight aggregate. The Stokes radius of the monomer, determined either from the diffusion coefficient or by combining the sedimentation equilibrium data with the sedimentation velocity data, was 94 Å. The frictional ratio was 2.2, suggesting a highly asymmetric or random coil structure. In the electron microscope, recombinant apolipoprotein(a) was visualized as a long, highly flexible chain of domains forming large, open coiled structures on the EM grid with contour lengths of about 800 Å. Addition of 6-aminohexanoic acid at 50 mM, a concentration which should saturate the weak lysine binding sites, did not alter the sedimentation behavior. In vivo, apolipoprotein(a) is associated tightly with LDL to form a highly atherogenic lipoprotein, Lp(a). A single molecule of recombinant apo(a) also associated tightly with LDL to yield a 13.3-S Lp(a)-like complex. This complex dissociated upon the addition of 50 mM 6-aminohexanoic acid. A novel sucrose gradient centrifugation technique was employed to determine a dissociation constant for the reversible equilibrium between recombinant apo(a) and LDL; at physiological ionic strength the dissociation constant was 0.3 nM. Raising the salt concentration to 5 M NaBr caused the dissociation constant to increase to 500 nM. Hydrodynamic modeling suggests recombinant apo(a) made contact with the LDL through, at most, a few kringles, with the remainder of the molecule extending into solution. Our results suggest that, in addition to the apoB–apo(a) disulfide bond, strong noncovalent forces hold the Lp(a) molecule together. Furthermore, the bulk of apo(a) is extended away from the lipoprotein surface, where it may readily interact with other ligands.

Recent studies (Durrington et al., 1988; Woo et al., 1991; Sandholzer et al., 1992; Seed et al., 1990) continue to support previous epidemiological evidence [reviewed in Loscalzo (1990)] implicating high plasma concentrations of lipoprotein-(a) [Lp(a)] as an important risk factor in the development of atherosclerosis, motivating investigation of the structure and genetics of apolipoprotein(a) [apo(a)] (Berg, 1990; Drayna et al., 1988; Utermann, 1989; Fless et al., 1986; McLean et al., 1987; Lackner et al., 1991) and the structure and function of its complex with LDL, Lp(a) (Fless et al., 1986; Gaubatz et al., 1983; Utermann & Weber, 1983; Fless et al., 1984; Fless et al., 1985; Kraft et al., 1992). Apo(a) isolated from plasma Lp(a) has been difficult to study, however, because of the existence of multiple high molecular weight isoforms (Utermann, 1989; Lackner et al., 1991; Scanu & Fless, 1990) and also due to the covalent attachment of the apo(a) through disulfide bonds to LDL (Fless et al., 1985). Reduction of these disulfides also results in reduction of the intrakringle disulfides, leading to a denatured and aggregated product.

Recombinant apo(a) [r-apo(a)], expressed and secreted in human embryonic kidney cells (293s cells) as a soluble protein (Koschinsky et al., 1991), provides a homogeneous, undenatured glycoprotein convenient to study by electron microscopy and conventional hydrodynamic techniques. Moreover, its interactions with LDL can be examined by these same techniques.

r-Apo(a), beginning at the N-terminus, contains 17 consecutive plasminogen type 4-like kringle domains followed by a single type 5-like kringle and a single protease-like domain at the C-terminus. The polypeptide molecular mass is calculated to be 249 000 Da, and as it has been measured to be 23% carbohydrate (Koschinsky et al., 1991), the monomeric glycoprotein molecular mass should be 323 000 Da.

In this paper we report measurement of some of the fundamental hydrodynamic parameters for recombinant

† This research was supported by a research grant from the National Institutes of Health (GM13914).

* Author to whom correspondence should be addressed.

0006-2960/93/0432-3722$04.00/0

apolipoprotein(a) in its native form and examine its structure in the electron microscope. We also report that, upon addition to human LDL, recombinant human apo(a) forms a very tight but reversible and, therefore, noncovalent, one-to-one complex with human LDL.

MATERIALS AND METHODS

Recombinant apo(a). Construction of the stable expression system for recombinant apo(a) [r-apo(a)] in 293s (human embryonic kidney) cells and the isolation and purification of the recombinant protein have been described (Koschinsky, et al., 1991). Recombinant apo(a) was frozen and shipped on dry ice to UCLA, where it was thawed, aliquoted, quick-frozen with liquid nitrogen, and stored at −20 °C until used.

Low-Density Lipoproteins. Low-density lipoproteins (LDL) were isolated in the density range 1.020–1.055 g/mL by sequential flotation. Blood was drawn into 10-mL Vacutainers (Becton-Dickson, Rutherford, NJ) containing EDTA as an anticoagulant. A 100× protease inhibitor cocktail was immediately added to the blood to give final concentrations of 24 μg/mL Polybrene, 2 mM benzamidine, 5 mM ε-aminocaproic acid, and 10 μg/mL soybean trypsin inhibitor (Sigma). Plasma was then isolated by low-speed centrifugation in a clinical centrifuge and made 0.04% in EDTA, 0.05% in sodium azide, and 0.005% in gentamicin using stock solutions of 4%, 5%, and 1%, respectively. These stock solutions were used to maintain the concentrations of EDTA, sodium azide, and gentamicin throughout the isolation. The plasma was adjusted to a density of 1.063 g/mL with a 25% NaCl stock solution and centrifuged in polycarbonate bottles in the Ti70.1 rotor for 20 h at 44 000 rpm and 20 °C in an L5-65 ultracentrifuge (Beckman Instruments, Inc., Palo Alto, CA). The top milliliter of each tube, which contained VLDL, IDL, and LDL, was removed. The density of the pooled fraction was adjusted to 1.020 g/mL with 25% NaCl, and centrifugation was repeated as before. The top milliliter of the solution, which contained VLDL and IDL, was removed. The next 7 mL of each tube was removed and discarded, and the LDL pellet was gently resuspended in the remaining milliliter. The LDL solution was then adjusted to a density of 1.055 g/mL with 25% NaCl; centrifugation was repeated as before, and the LDL was isolated in the top 0.5–1 mL of the tube.

Hydrodynamic Measurements. Sedimentation velocity and diffusion measurements were made using a Beckman Model E analytical ultracentrifuge equipped with a mirror optical system, xenon light source, photoelectric scanner, and multiplexer. The scanner pen voltage was amplified and fed to an 8-channel, 12-bit A/D converter and timer/counter board (Omega Engineering, Inc., Stamford, CT) installed in an EST Premium/286 personal computer with a math coprocessor. Digitized scans were stored on floppy disks, and subsequent data analysis was performed on a VAX cluster consisting of 3 VAXstation 3100's. Sedimentation coefficient distribution plots for Figure 5 were produced by taking the derivative of individual scans, multiplying each point by a radius-cubed weighting factor, and converting the horizontal axis from distance in the ultracentrifuge cell to sedimentation rate (Schumaker & Schachman, 1957).

Samples used for diffusion analysis were further purified by sucrose gradient ultracentrifugation. r-apo(a) (0.2 mL) in PBS was layered atop a 3.8-mL linear 5–20% sucrose gradient in a polyallomer SW60 tube and spun in the SW60 rotor for 5.5 h at 48 000 rpm at 20 °C in a L5-65 ultracentrifuge (Beckman Instruments, Inc., Palo Alto, CA). The gradient was subsequently fractionated into 0.25-mL fractions with an ISCO Model 640 density gradient fractionator equipped with a UA-5 absorbance fluorescence monitor (ISCO, Lincoln, NE). Diffusion coefficients were determined at low speeds (6000–6600 rpm) in the analytical ultracentrifuge using synthetic boundary cells and the ANF titanium rotor. The boundary formed was stabilized by the inclusion of 0.5% sucrose in the sample solution. Data analysis was performed as previously described (Elovson et al., 1985).

Sedimentation equilibrium measurements were made using a Beckman Optima XLA analytical ultracentrifuge. All samples were loaded into 6-channel equilibrium cells equipped with charcoal-filled Epon centerpieces. The sedimentation data were analyzed using both single ideal species and two ideal species models. The absorbance, A_r, at any radial position, r, is related to the molecular weights, M_1 and M_2, of species 1 and 2, by

$$A_r = \sum_{i=1}^{2} A_{i,r} \exp[(\omega^2/RT) M_i (1 - v_i\rho)(r^2 - r_0^2)] \quad (1)$$

where $A_{i,r}$ is the absorbance of species i at a radial reference distance r_0; ω, the angular velocity; R, the gas constant; T, the Kelvin temperature; v_i, the partial specific volume of species i; and ρ, the solution density. The reference radial distance, r_0, for the analysis was set to a radial position $^2/_3$ of the column height. The data were fitted to this equation with the general curve fitting routines in the commercially available graphics software package KaleidaGraph.

Electron Microscopy. A 10-mL drop of 10–20 μg/mL r-apo(a) was placed on a freshly glow-discharged carbon-, or carbon–parlodion-covered copper grid, and macromolecules were allowed to adhere for 1 min. The drop was then removed by touching a filter paper wedge (Whatman No. 4) to the edge of the grid. The still-wet grid was washed with five successive drops of 1% aqueous uranyl acetate. A sixth drop of uranyl acetate was left on the grid for 45 s and then removed by touching a wet filter paper wedge to the edge of the grid. The grid was placed face up on filter paper (Whatman No. 1) in a Petri dish, allowed to air dry, and stored in a dessicator. All grids were examined within 1 day of preparation.

Grids were examined in a Hitachi H-7000 electron microscope operating at 75 kV with a 200-μm condenser aperture and a 50-μm objective aperture.

Determination of Dissociation Constants. A novel sucrose gradient centrifugation technique was employed to measure dissociation constants at physiological ionic strength in PBS. In this technique, zones of ^{125}I-labeled r-apo(a) were centrifuged through sucrose gradients containing various concentrations of LDL uniformly distributed throughout the initial gradients. The LDL boundary floated slowly up from the bottom while the zone containing r-apo(a) and the r-apo(a)–LDL complex with which it was in equilibrium migrated down from the top in the presence of the LDL. The sedimentation rate of the zone of radiolabeled r-apo(a) would then be a function of how much time individual molecules of r-apo(a) spent in the bound form, which was determined by the K_d and the LDL concentration. A plot of the position of the radiolabeled r-apo(a) peak versus LDL concentration gave the dissociation constant, determined as the LDL concentration at the midpoint of the curve. Centrifugation was stopped before the floating boundary of the LDL passed the sedimenting zone of r-apo(a). Linear sucrose gradients from 8.5 to 20% (w/v) in 150 mM sodium chloride, 1 mg/mL nonspecific human γ-globulin (Sigma) carrier, and 10 mM sodium phosphate, pH 7.4, were prepared, containing uniform

concentrations of LDL as indicated. Fifty-microliter aliquots containing a trace concentration of recombinant apo(a) labeled with Bolton–Hunter reagent (Amersham) to 10^8 cpm/μg was added to the top of each tube. The gradients were spun at 52 000 rpm for 165 min at speed, with 30 min acceleration and 30 min deceleration. Under these conditions, unbound apo(a) migrates 18 mm from the top of the tube, while the 1:1 apo(a)–LDL complex migrates 10 mm. Fractions (100 μL, 1.4 mm) were collected from the top and counted to locate the peak position of the radiolabeled recombinant apo(a).

For the experiments performed at elevated NaBr concentration, various concentrations of LDL and a tracer concentration of recombinant human apo(a) were mixed and centrifuged together in 5 M sodium bromide, 0.2% BSA (Sigma, RIA grade), and 1 mM phosphate, pH 7.0. The samples were loaded into Beckman Ultraclear 5 × 41 mm centrifuge tubes and placed in a SW65 rotor fitted with adaptors. Centrifugation was for 1.75 h at 45 000 rpm. Under these conditions, the LDL moved rapidly to the top, the recombinant apo(a) did not sediment appreciably, and the complex moved toward the top at an intermediate rate. At the conclusion of the centrifugation, the bottom half of the tube contents was withdrawn through a syringe. Samples were counted in triplicate using the Beckman Gamma 7000 counter. The extent of depletion of the bottom half of the tube was plotted as a function of the logarithm of the LDL concentration.

RESULTS

Sedimentation. Recombinant apo(a) was initially studied by analytical ultracentrifugation, and careful examination of the shape of the sedimenting boundaries revealed evidence of heterogeneity. Figure 1A shows consecutive scanner traces of a solution of recombinant apo(a) which appeared homogeneous by SDS gel electrophoresis. Sedimentation heterogeneity was obvious even in the early scans as a forward skewing at the leading edge, and with the passage of time, the boundary resolved into two components: a major, well-defined, slower sedimenting monomer and a minor, broader, faster polymer. The percentage of polymer did not appear to change as the concentration was reduced over a 30-fold range, suggesting that the polymer was a stable contaminating species. A careful study of the sedimentation velocity over a concentration range between 10 and 280 μg/mL was performed to yield a plot of $s_{20,w}$ vs concentration, which extrapolated to a value of $s_{20,w}$ = 9.30 S for the monomer (Figure 1B). A value of $s_{20,w}$ = 12–13 S was estimated for the polymer.

Diffusion. Prior to measurment of the diffusion coefficient, the recombinant apo(a) sample was purified on a sucrose gradient in an attempt to remove contaminating polymer, as described in Materials and Methods. The diffusion coefficient, D, of recombinant apo(a) was conveniently measured in the ultracentrifuge at a relativity low rotor speed (6400 rpm), using the centrifugal field to stabilize the diffusing boundary formed near the center of a synthetic boundary cell by layering solvent over a protein solution during acceleration of the ultracentrifuge rotor. Figure 2A shows plots of absorbance vs radius for consecutive scans at 8-min intervals. These same data were analyzed by the probit analysis shown in Figure 2A; the slopes of the straight lines yielded $2Dt$. An uncertainty in the initial time was eliminated by plotting $2Dt$ as a function of t (Figure 2B); the slope yielded $2D$.

From the measured value of the diffusion coefficient, 2.29 F, the Stokes radius may be calculated as 93.6 Å (Table I).

Partial Specific Volume. If the partial specific volume is known, the molecular weight may be calculated from the sedimentation and diffusion coefficients; conversely, if the molecular weight is known, the partial specific volume may be calculated from the same data.

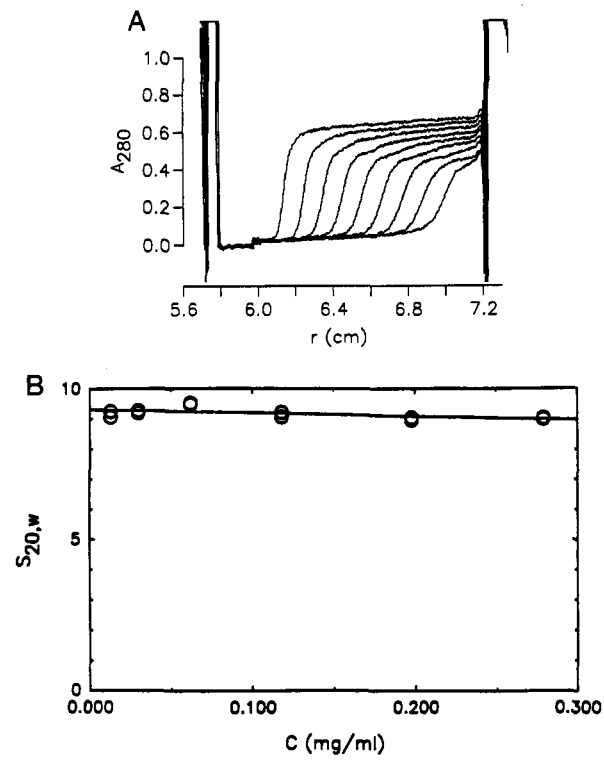

FIGURE 1: (A) Sedimentation profile. Consecutive scanner traces of the migrating boundary of a solution of recombinant apo(a) show a homogeneous monomeric component and 15–20% of dimer and higher aggregates. Run conditions: 48 000 rpm, 20.8 °C, 8-min scanner intervals, 0.15 M NaCl, and 0.015 M sodium phosphate, pH 7.4. (B) Concentration dependence. Sedimentation coefficients, corrected for temperature and the density and viscosity of the solvent, are plotted as a function of protein concentration to yield $s^0_{20,w}$.

Initially, an attempt was made to determine the partial specific volume from measurements of the sedimentation coefficient as a function of solvent density, using D_2O to increase solvent density over the range between 1.00 and 1.09 g/mL. The long extrapolation yielded 0.66 ± 0.03 mL/g (95% confidence interval). Together with s and D, a molecular weight of 290 000 was calculated for the monomer (Table I). This value for the molecular weight of the recombinant Lp(a) monomer seemed low; since the protein portion contributed 249 000, the increment in molecular weight would correspond to a carbohydrate content of 16.5%, which is considerably below the reported value of 23% (Koschinsky et al., 1991). Moreover, 16.5% is too little carbohydrate to drop the partial specific volume to 0.66 mL/g, since the calculated value, based upon the amino acid sequence and a carbohydrate content of 23%, is only 0.687 mL/g.

Alternatively, it is possible to determine the partial specific volume from s and D, assuming a molecular weight of 323 000, which corresponds to 23% carbohydrate. This value, 0.69 mL/g, agrees with the 0.687 mL/g calculated from the amino acid composition and carbohydrate content.

Sedimentation Equilibrium. Nine independent measurements of molecular weight by sedimentation equilibrium using four different preparations of recombinant apo(a) were performed (Table II). Raw data from one such experiment is shown in Figure 3A as a plot of absorbancy at 280 nm versus radial position after 60 h of centrifugation at 20 °C. A nonlinear least squares procedure, assuming a single molecular weight species, gave an average value of 359 000,

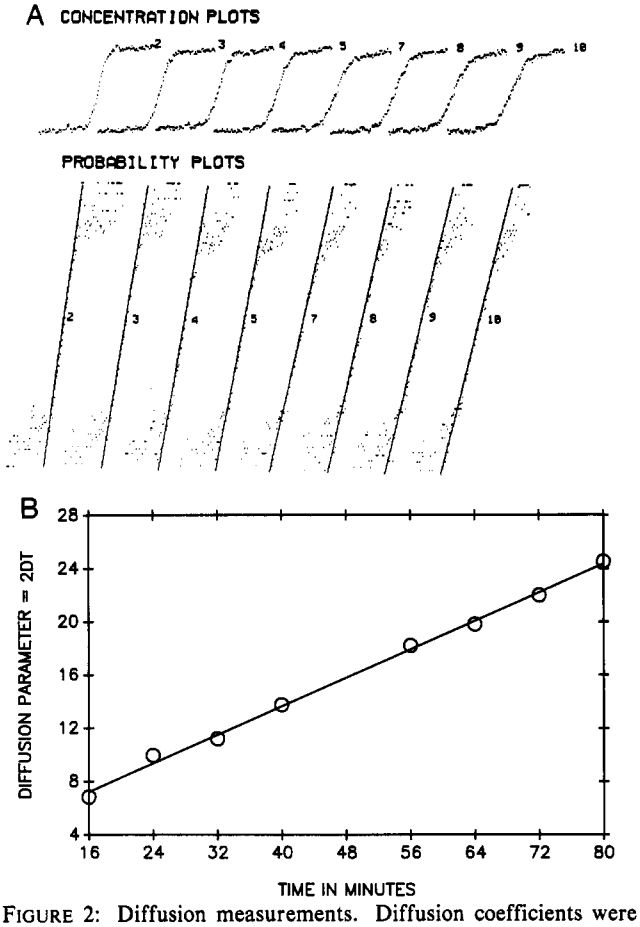

FIGURE 2: Diffusion measurements. Diffusion coefficients were determined using a synthetic boundary cell in the analytical ultracentrifuge. (A) The upper panel shows scanner traces of the diffusing boundary of a sample of recombinant apo(a) monomer purified on a sucrose gradient. The lower panel shows these same data converted to probability (probit) plots. Also shown are the superimposed least squares straight lines calculated from the data points lying between the 30 and 70% concentration limits; from the slopes of these lines, values of $2Dt$ are calculated. (B) A plot of the $2Dt$ values as a function of time, t, yields a diffusion coefficient of 2.23 ficks. Run conditions: 6400 rpm, 20–20.5 °C, protein concentration 0.05 mg/mL, wavelength 230 nm.

Table I: Hydrodynamic Data

$s^0_{20,w}$	9.30 S
$D_{20,w}$	2.29 ficks
partial sp vol	0.69 mL/g (measd)[a]
	0.69 mL/g (calcd)[b]
MW from s and D	320 000 g/mol
MW from sed equil	96% 325 000 ± 10 000
	4% 1 300 000 ± 200 000
	(SEM, n = 8)
Stokes' radius	94 Å[c]
f/f_0	2.2

[a] From s and D or from sedimentation equilibrium, assuming a molecular weight of 323 000 (23% carbohydrate). [b] Calculated from amino acid and carbohydrate composition. [c] The same value is obtained independently from the diffusion coefficient or from the sedimentation equilibrium molecular weight and the sedimentation coefficient.

a number which differs significantly from 323 000. A two-component, nonlinear least squares fit yielded an average monomer molecular weight of 325 000 for the major component and 1 300 000 for the minor component. The percentage of monomer present varied somewhat, depending on the apo(a) preparation used and details of the fitting procedure, but was greater than 90%. (One data point, obviously too high, was excluded from the calculation of the average values listed in Table I.)

Table II: Sedimentation Equilibrium of Apo(a)

lot	cell	single ideal species	two ideal species MW1	%	MW2	%
1	1A	398 000	334 000	97	1 900 000	3
	1B	330 000	304 000	96	1 100 000	4
	1C	340 000	295 000	92	900 000	8
2	1C	312 000	296 000	94	700 000	6
	3A	377 000	361 000	99.5	2 200 000	0.5
3	2A[a]	484 000	445 000	97.8	1 800 000	2.2
	3B	368 000	318 000	95.6	1 500 000	4.4
4	1B	365 000	332 000	95.7	1 300 000	4.3
	2C	382 000	362 000	97.6	1 100 000	2.4
Averages[a]		359 000	325 000	95.7	1 300 000	4.3

[a] Data from cell 2A was not included in calculating the average values listed above.

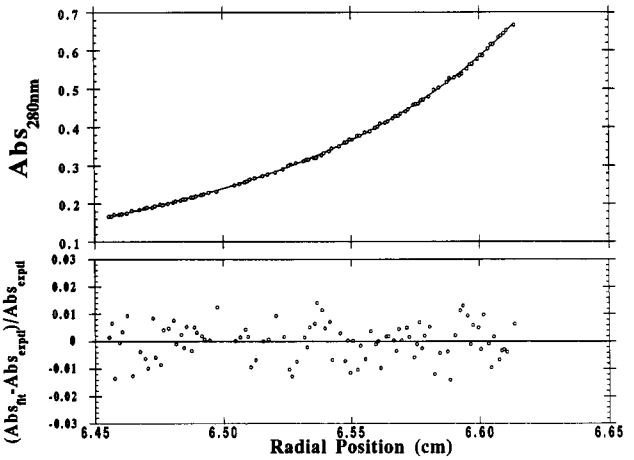

FIGURE 3: Sedimentation equilibrium. Concentration profile after centrifugation for 60 h at 4 °C and 5000 rpm, at an initial concentration of 400 μg/mL (Lot 4, cell 1 B). The absorbance is plotted as a function of radial distance. The data are analyzed to yield the best two-component fit, in this case shown as the line through the experimental points; 95.7% of the material is present as a "monomer" with a molecular mass of 332 000 Da, and 4.3% is present as "polymer" with a molecular mass of 1 300 000 Da.

If the glycoprotein is assumed to have a molecular weight of 323 000 (23% carbohydrate), then the partial specific volume may be calculated from the sedimentation equilibrium data, yielding a value of 0.684 mL/g.

Using the molecular weight obtained from sedimentation equilibrium and the sedimentation coefficient, an estimate of the Stokes radius independent of the diffusion coefficient yields 93.8 Å.

Electron Microscopy. Recombinant apo(a) was visualized with the electron microscope, using a negative strain to provide contrast (Figure 4). A long, flexible molecule with a contour length of approximately 800 Å was seen, and careful inspection revealed a chain of multiple domains. In some of the better images the chain was resolved into about 17–18 smaller domains, terminating in a larger domain.

LDL Binding Studies. In order to explore the interaction between r-apo(a) and LDL, a series of experiments were performed in which 7.0-S LDL and 9.3-S recombinant apo-(a) were mixed in PBS and studied by analytical ultracentrifugation. The major component sedimented at 13.3 S, approximating the value calculated for the 1:1 heterodimer of apo(a) and LDL (see Discussion). The addition of an excess of either LDL or apo(a) above equimolarity showed the presence of the corresponding slower component, clearly demonstrating that the faster component was not a 2:1 or a 1:2 complex. In high apo(a) excess, however, the major peak moved even faster, suggesting further weak complexation,

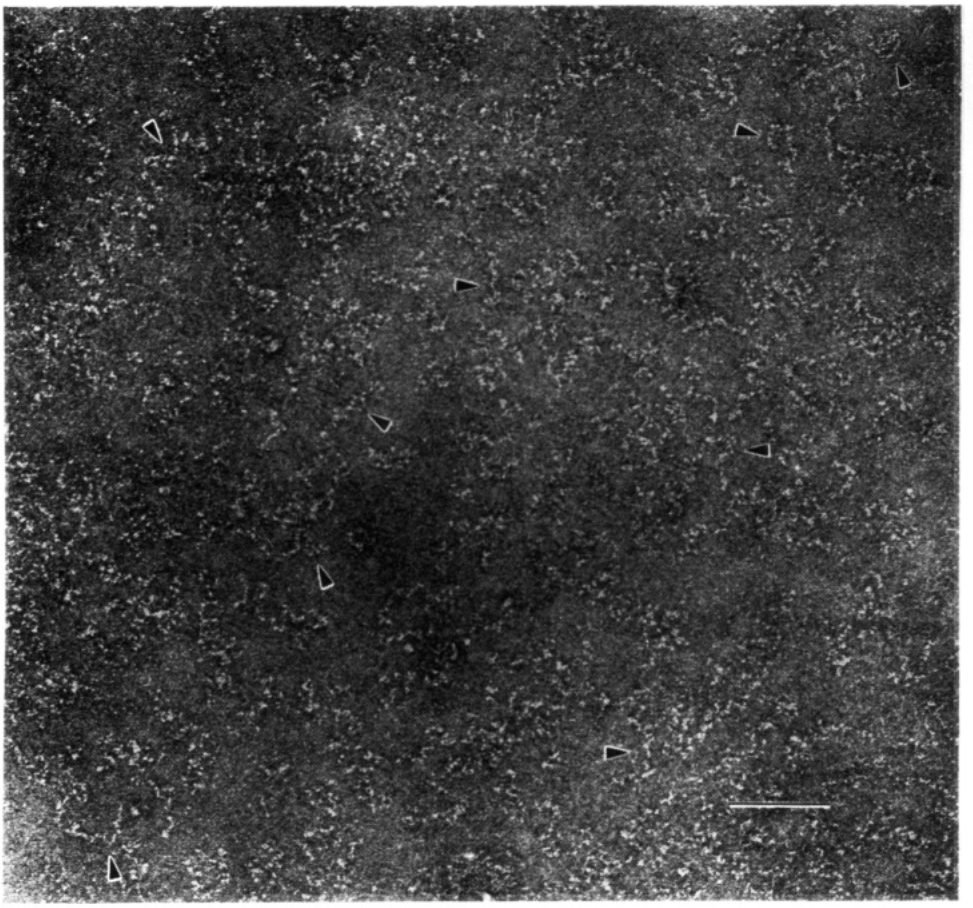

FIGURE 4: Electron microscopy. Recombinant apo(a) was adsorbed to a carbon–coated EM grid as described in Materials and Methods and negatively stained with uranyl acetate. This field shows recombinant apo(a) densely packed but with clearly distinguishable individual coiled molecules. The arrowheads indicate several such molecules. The bar corresponds to 1000 Å.

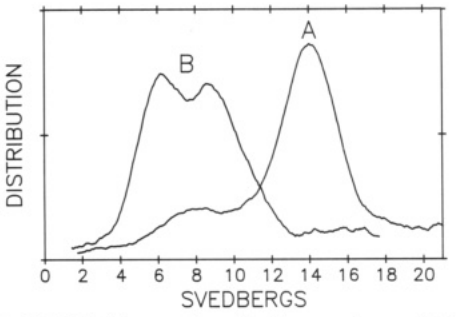

FIGURE 5: LDL binding studies. Sedimentation coefficient distributions of (A) a mixture of LDL and r-apo(a) with the r-apo(a) in approximately 2.3-fold molar excess and (B) the same mixture after addition of 50 mM 6-aminohexanoic acid and recentrifugation.

although it was not possible to determine a second binding constant. Thus, in Figure 5, curve A, a 14-S complex peak moved ahead of a broad 9-S peak of excess apo(a).

Upon addition of 50 mM 6-aminohexanoic acid and recentrifugation of the resuspended mixture of LDL and recombinant apo(a), the complex dissociated to regenerate the LDL, which because of its low density runs at 6.0 S in this buffer, and the 9.3-S recombinant apo(a) (Figure 5, curve B). In a control experiment the sedimentation coefficient of the recombinant apo(a) was unchanged by 50 mM 6-aminohexanoic acid.

The lack of covalent attachment between recombinant apo(a) and LDL has also been checked by SDS–PAGE under nonreducing conditions. A mixture of LDL and apo(a), even after incubation for 2 weeks at 4 °C, separated into two separate bands in nonreducing SDS gels, precluding the spontaneous formation of a disulfide bond under these conditions (data not shown).

Sucrose gradient studies were also performed to determine the K_d for the reversible binding between recombinant apo(a) and LDL; as shown in Figure 6a, a value of 0.3 nM was found for human LDL at physiological ionic strength and 20 °C. In a concentrated NaBr solution, the value of K_d was 500 nM, suggesting that the interaction is primarily ionic in nature (Figure 6b).

DISCUSSION

The apparent molecular mass of recombinant apo(a) on SDS–PAGE under reducing conditions is 500 kDa (Koschinsky et al., 1991). Since we have demonstrated that the large majority of apo(a) molecules in solution are in the monomeric form, this estimated molecular weight is a reflection of the anomalously high molecular weights frequently seen for heavily glycosylated proteins. It is not unreasonable to suggest that this is also probably true for plasma apo(a), which has apparent molecular masses ranging from 280 to 800 kDa as estimated by SDS–PAGE (Scanu & Fless, 1990). The actual values are probably considerably less, perhaps only two-thirds of the values estimated on reducing gels.

One advantage of working with recombinant apo(a) is that is has not been subject to reduction. In contrast, plasma apo(a) is isolated from Lp(a) by reduction and alkylation, leading to an aggregated and denatured product. Physical studies on denatured apo(a) have required a strongly chaotropic solvent, such as guanidinium HCl, to prevent aggregation. Thus, 6 M guanidinium HCl was required as a solvent in sedimentation equilibrium studies to determine the molecular mass of one

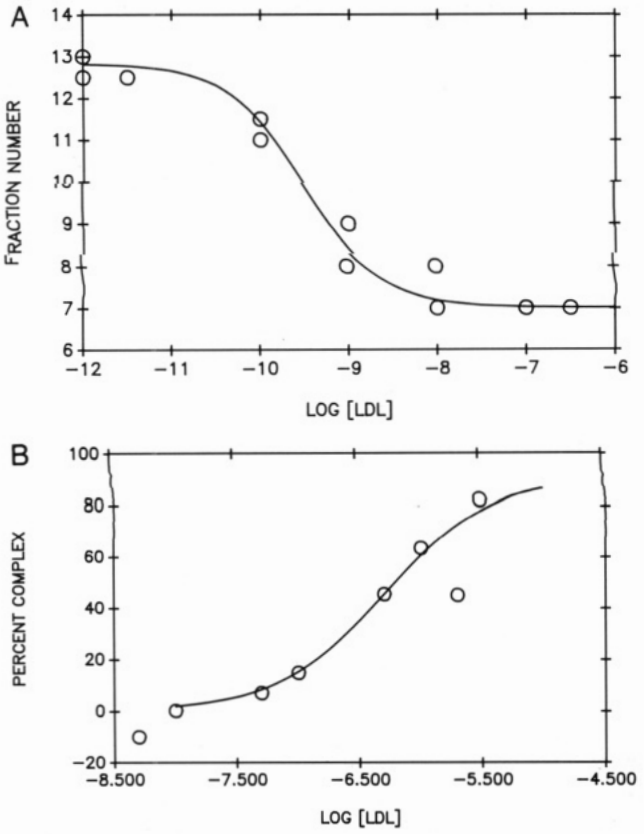

FIGURE 6: Measurement of the dissociation constants between recombinant apo(a) and human LDL. (A) Sucrose gradient centrifugation was employed to measure the interaction between various concentrations of LDL uniformly distributed throughout the initial gradient and a zone of ^{125}I-labeled recombinant human apo(a). The position of the r-apo(a) peak (fraction number from the top) is plotted as a function of the LDL concentration. The dissociation constant is the LDL concentration at the midpoint of the curve. (B) Flotation of recombinant apo(a) bound to LDL is determined in this experiment, where a tracer quantity of labeled, recombinant apo(a) is mixed with LDL uniformly dispersed in a solution containing 5 M NaBr. Plotted is the depletion of the radiolabeled r-apo(a)–LDL complex from the bottom half of the tube after centrifugation, as a function of LDL concentration. The LDL concentration at the midpoint is the estimated dissociation constant.

sample of plasma apo(a) as 281 000 Da (Fless et al., 1986).

From the electron micrographs, recombinant apo(a) was seen to be a flexible molecule of about 800 Å in length and composed of a string of 19 domains. Thus, an average domain spacing of 800/19 = 42.1 Å/domain can be estimated. The kringle domain in the tissue plasminogen activator has been crystallized, and its three-dimensional structure has been described (de Vos et al., 1992). The kringle is an oblate ellipsoid with approximate dimensions of 28 × 30 × 11 Å.[3] In r-apo(a) there would appear to be a length of chain of approximately 36 residues between kringles which could extend the spacing between kringles to 42.1 Å and provide flexibility. The Stokes radius, R_e, of the recombinant apo(a) may be determined from the translational frictional coefficient, and the radius of gyration, R_G, of the corresponding random coil may be determined from the expression $R_e = 0.665R_G$, as described by Tanford (1961). This yields an observed value for the radius of gyration of R_G = 141 Å. A completely flexible random coil composed of 19 uniform elements, each with a length of 42.1 Å, would have a calculated radius of gyration of 74.9 Å, as described by eqs 9–8 and 9–38 of Tanford (1961). That this calculated value is less than the observed radius of gyration of 141 Å suggests that flexibility is restricted between

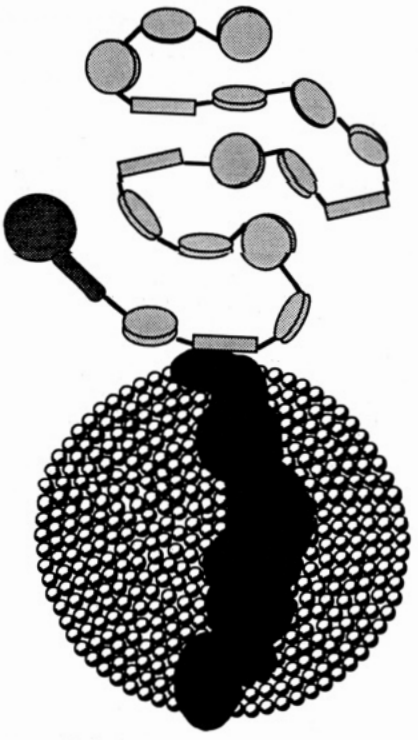

FIGURE 7: A model for recombinant Lp(a). Hydrodynamic studies suggest that recombinant apo(a) is attached at one kringle to LDL, leaving the bulk of the molecule extending into solution, where it provides frictional resistance to sedimentation.

elements of the chain. To estimate the degree of restriction, we used a model in which flexibility is limited, so that the angle between successive elements is θ, although free rotation is permitted around the axis of each element. This model is described by eq 9–11 of Tanford (1961) and predicts that when $\theta = 52°$ for a chain of 19 elements of 42.1-Å length, the radius of gyration will be approximately 141 Å.

When recombinant apo(a) binds to the LDL, the sedimentation coefficient of the complex increases from $s_{20,w}$ = 7.0 S for the LDL and 9.3 S for apo(a) to 13.3 S for the complex. It was interesting to analyze this increase in terms of the increase in the frictional ratio of the LDL upon binding apo(a). Two extreme cases are considered: in the first, recombinant apo(a) is uniformly layered over the surface of the LDL, increasing the hydrodynamic radius of the LDL and decreasing its partial specific volume, but not changing its frictional ratio, f/f_0. In this case, calculation predicts that the spherical complex would have a sedimentation coefficient of 15.8 S, much larger than the observed value of 13.3 S. In the second case, the complex is composed of a single molecule of apo(a) in the form of a hydrodynamic random coil, attached at a single point to the LDL. Thus, the frictional properties of the complex were those of two touching spheres of 104 Å, the approximate Stokes radius of an LDL (Chapman et al., 1988), and 94 Å, the Stokes radius of apo(a). If the two spheres had equal radii, hydrodynamic theory would predict a sedimentation coefficient of 12.2 S (Cantor & Schimmel, 1980), a little less than the 13.3 S actually observed. These results suggest that the recombinant apo(a) is attached to the LDL at one kringle, or at most a few kringles, leaving the bulk of the r-apo(a) extending out into the solution, where it provides frictional resistance to sedimentation (Figure 7).

As an LDL contains approximately 800 phospholipid molecules, the 1:1 complex is unlikely to represent r-apo(a) binding to phospholipid. Phospholipid binding may, however, play a role in the additional, much weaker binding seen in

high r-apo(a) excess. The mode of attachment between the LDL and recombinant apo(a) is noncovalent, since it is readily reversed by 50 mM 6-aminohexanoic acid. The aspartic acid of plasminogen implicated in fibrin binding (Trexler et al., 1982) is present in only one of the kringle 4-like domains of apo(a) (McLean et al., 1987), the 17th kringle 4-like domain of r-apo(a). This kringle may be involved in the 6-aminohexanoic acid dissociable interaction between r-apo(a) and LDL. Sucrose gradient sedimentation studies measure a K_d = 0.3 nM for the attachment between recombinant apo(a) and human LDL at physiological ionic strength; strong noncovalent association has previously been reported between recombinant apo(a) and human LDL (Trieu et al., 1991). The interaction appears to be principally ionic in nature, for the affinity decreases by over 3 orders of magnitude when 5 M NaBr is employed instead of 0.15 M NaCl.

It seemed possible that prolonged attachment in an air-saturated solution could cause spontaneous formation of a disulfide link. Disulfide linkage between recombinant apo(a) and apoB has been reported for the Lp(a)-like molecules secreted by transfected HepG2 cells (Koschinsky et al., 1991). Even after 2 weeks of incubation at 4 °C of a noncovalent complex of recombinant apo(a) and LDL, however, no covalent attachment of the recombinant apo(a) to apoB was observed by SDS–PAGE. One of the kringles of r-apo(a), kringle 16, contains an additional cysteine beyond those which should be involved in intrakringle disulfide bonds. Although purified r-apo(a) is not disulfide-linked to other proteins, we do not, strictly speaking, know that this cysteine is free.

In conclusion, recombinant apo(a) has been studied by hydrodynamic and EM techniques. In solution, the molecule may be modeled as a random coil with limited flexibility between kringles. Recombinant apo(a) forms a tight, noncovalent complex with LDL by attachment at one or, at most, a few points, leaving the bulk of the apo(a) in the form of a random coil. This complex dissociates in the presence of 50 mM 6-aminohexanoic acid.

REFERENCES

Berg, K. (1990) in *From Phenotype to Gene in Common Disorders* (Berg, K., Retterstol, N., & Refsum, S., Eds.) pp 138–162, Munksgaard, Copenhagen.

Cantor, C. R., & Schimmel, P. R. (1980) *Biophysical Chemistry. Part II: Techniques for the study of biological structure and function*, Vol. II, p 569, W. H. Freeman and Company, San Francisco.

Chapman, M. J., Laplaud, P. M., Luc, G., Forgez, P., Bruckert, E., Goulinet, S., & Lagrange, D. (1988) *J. Lipid Res. 29*, 442–458.

de Vos, A. M., Ultsch, M. H., Kelley, R. F., Padmanabhan, K., Tulinsky, A., Westbrook, M. L., & Kossiakoff, A. A. (1992) *Biochemistry 31*, 270–279.

Drayna, D. T., Hegele, R. A., Hass, P. E., Emi, M., Wu, L. L., Eaton, D. L., Lawn, R. M., Williams, R. R., White, R. L., & Lalouel, J. M. (1988) *Genomics 3*, 230–236.

Durrington, P. N., Ishola, M., Hunt, L., Arrol, S., & Bhatnagar, D. (1988) *Lancet 1* (May 14, No. 8594), 1070–1073.

Elovson, J., Jacobs, J. C., Schumaker, V. N., & Puppione, D. L. (1985) *Biochemistry 24*, 1569–1578.

Fless, G. M., Rolih, C. A., & Scanu, A. M. (1984) *J. Biol. Chem. 259*, 11470–11478.

Fless, G. M., ZumMallen, M., & Scanu, A. M. (1985) *J. Lipid Res. 26*, 1224–1229.

Fless, G. M., ZumMallen, M., & Scanu, A. M. (1985) *J. Biol. Chem. 261*, 8712–8718.

Gaubatz, J. W., Heideman, C., Gotto, A. M., Jr., Morriset, J. D., & Dahlen, G. H. (1983) *J. Biol. Chem. 258*, 4582–4589.

Kraft, H. G., Sandholzer, C., Menzel, H. J., & Utermann, G. (1992) *Arterioscler. Thromb. 12*, 302–306.

Koschinsky, M. L., Tomlinson, J. E., Zioncheck, T. F., Schwartz, K., Eaton, D. L., & Lawn, R. M. (1991) *Biochemistry 30*, 5044–5051.

Lackner, C., Boerwinkle, E., Leffert, C. C., Rahmig, T., & Hobbs, H. H. (1991) *J. Clin. Invest. 87*, 2153–2161.

Loscalzo, J. (1990) *Arteriosclerosis (Dallas) 10*, 672–679.

McLean, J. W., Tomlinson, J. E., Kuang, W.-J., Eaton, D. L., Chen, E. Y., Fless, G. M., Scanu, A. M., & Lawn, R. M. (1987) *Nature 330*, 132–137.

Sandholzer, C., Boerwinkle, E., Saha, N., Tong, M. C., & Utermann, G. (1992) *J. Clin. Invest. 89*, 1040–1046.

Scanu, A. M., & Fless, G. M. (1990) *J. Clin. Invest. 85*, 1709–1715.

Schumaker, V. N., & Schachman, H. K. (1957) *Biochim. Biophys. Acta 23*, 628–639.

Seed, M., Hoppichler, F., Reaveley, D., McCarthy, S., Thompson, G. R., Boerwinkle, E., & Utermann, G. (1990) *New England J. Med. 322*, 1494–1499.

Tanford, C. A. (1961) *Physical Chemistry of Macromolecules*, pp 156, 158, 167, and 362, John Wiley & Sons, New York.

Trexler, M., Vali, Z., & Patthy, L. (1982) *J. Biol. Chem. 257*, 7401–7406.

Trieu, V. N., Zioncheck, T. F., Lawn, R. M., & McConathy, W. J. (1991) *J. Biol. Chem. 266*, 5480–5485.

Utermann, G. (1989) *Science 246*, 904–910.

Utermann, G., & Weber, W. (1983) *FEBS Lett. 154*, 357–371.

Woo, J., Lau, E., Lam, C. W., Kay, R., Teoh, R., Wong, H. Y., Prall, W. Y., Kreel, L., & Nicholls, M. G. (1991) *Stroke 22*, 203–208.